regularized contour dynamical algorithm with a node insertion-and-removal algorithm.[11] The close agreement between the linear and nonlinear solutions validates the numerical algorithm.

[1]S. L. Ossakow, Rev. Geophys. Space Phys. 17, 521 (1979).

[2]L. M. Linson and J. B. Workman, J. Geophys. Res. 75, 3211 (1970).

[3]J. N. Shiau and A. Simon, Phys. Rev. Lett. 29, 16–64 (1972).

[4]H. J. Völk and G. Haerendel, J. Geophys. Res. 76, 4541 (1971).

[5]A. Simon, Phys. Fluids 6, 382 (1963).

[6]N. J. Zabusky, J. H. Doles, III, and F. W. Perkins, J. Geophys. Res. 78, 711 (1973). Also, J. H. Doles, III, N. J. Zabusky, and F. W. Perkins, J. Geophys. Res. 81, 5987 (1976).

[7]A. J. Scannapieco, S. L. Ossakow, D. L. Book, B. E. McDonald, and S. R. Goldman, J. Geophys. Res. 79, 2913 (1974). Also, A. J. Scannapieco, S. L. Ossakow, S. R. Goldman, and J. M. Pierre, J. Geophys. Res. 81, 6037 (1976).

[8]N. W. Rosenberg, J. Geophys. Res. 76, 6856 (1971); T. N. Davis, G. J. Romick, E. M. Wescott, R. A. Jeffries, D. M. Kerr, and H. M. Peek, Planet Space Sci. 22, 67 (1974); K. D. Baker and J. C. Ulwick, Geophys. Res. Lett. 5, 723 (1978).

[9]G. I. Marchuk, *Methods of Numerical Mathematics* (Springer-Verlag, New York, 1975), and references therein. See, in particular, 5.2 and 5.3.

[10]N. J. Zabusky and E. A. Overman, II, "Regularization of Contour Dynamical Algorithms" (unpublished).

[11]E. A. Overman, II, and N. J. Zabusky, "A Regularized Contour Dynamical Algorithm for the Evolution of Plasma Clouds and Deformable Dielectrics" (unpublished).

Time-Dependent Images in Transmission Electron Microscopy Associated with the Phase Transitions of $NbSe_3$

K. K. Fung and J. W. Steeds

H. H. Wills Physics Laboratory, University of Bristol, Royal Fort, Bristol BS8 1TL, England

(Received 3 June 1980)

Strandlike domains have been observed in $NbSe_3$ at temperatures below 144 K by imaging in one of the satellite reflections produced by the phase transition. These appear to twinkle rapidly with many strands in the field of view lighting up and switching off in periods of a few seconds. In addition, fringes along these strands have been observed.

PACS numbers: 64.70.Kb, 61.16.Di, 72.15.Nj

The unusual properties associated with the phase transitions of $NbSe_3$ at 144 and 59 K have aroused a great deal of interest.[1] In particular the non-Ohmic electrical conductivity observed near both these transitions has stimulated several investigations[2,3] but still requires a full explanation. The material grows in the form of blade-shaped whiskers with the unique axis (b) of the monoclinic unit cell along the whisker.[4] At each of the phase transitions incommensurate satellites appear in diffraction experiments with wave vector components along the b axis which differ slightly from $\frac{1}{4}b^*$.[5] It is generally accepted that the phase transitions are driven by charge-density-wave (CDW) instabilities and that the non-Ohmic conductivity results from unpinning of the charge density waves.[6] However, direct evidence for the unpinning is at present lacking and the detailed microstructure of the incommensurately modulated state is open to conjecture.

It is the purpose of this communication to report electron microscope observations which may be interpreted as direct evidence for the movement of CDW's and which indicate a stranded nature of the modulated state. These new results permit a reevaluation of a number of previous publications on $NbSe_3$ and lead to a proposal for the nature of the CDW state in this material.

The samples were grown by iodine vapor transport. They have a resistance ratio which is typically about 100:1. Thin foils were prepared from the whiskers for transmission electron microscopy (TEM) by cleavage and they were examined in a Philips EM400 electron microscope with a double-tilting liquid-helium–cooled stage designed by Dr. J. A. Eades and built in this laboratory. The samples were typically 50 nm thick. Temperature control is provided and it is possible to

achieve a thermal drift of less than 1 K/min. Absolute measurement of the temperature is difficult and has not been attempted yet. However, the nominal temperatures quoted hereafter are evidently not more than 10 K lower than the actual temperature of the irradiated region as can be judged from appearance and disappearance of diffraction satellites on cycling the specimen temperature. The samples were immersed in the objective lens field of approximately 1.8 T.

When the samples were investigated in the normal way, by bright field diffraction contrast electron microscopy, nothing unusual was observed. Attempts at dark field electron microscopy using an objective aperture which passed only a satellite reflection were initially unsuccessful because of the resulting very low image intensities. However, by tilting the whiskers so as to maximize the intensity of one or more satellite reflections and by using these to obtain satellite dark field (SDF) images it was discovered that the whiskers were broken up into fine dark and light strands approximately parallel to the whisker axis. Such images have been obtained from a wide variety of crystal orientations. Deviations of the strands from this direction by up to 15° were occasionally observed. The images sometimes revealed intensity modulations ("fringes") along the strands as illustrated in Fig. 1.

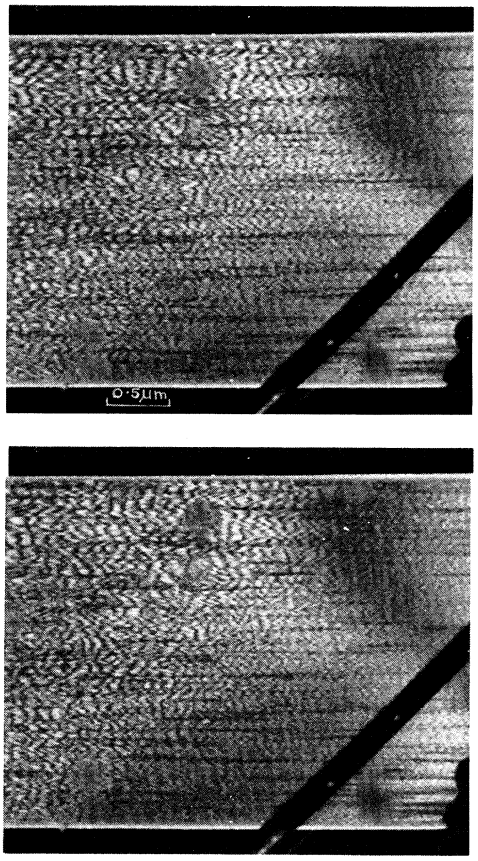

FIG. 1. Images revealing strands parallel to the whisker axis (right-hand sides of the micrographs) and trains of fringes within the strands (left-hand sides). The micrographs were two-second exposures taken with a time interval of approximately one minute. The dark band is the shadow of another whisker.

A number of interesting properties of these images have been noted. Perhaps the first and most telling point is that images such as those described above were only observed in satellite reflections; the effects are essentially associated with the phase transitions. Although strands were recorded in the satellites appearing at both the lower and the higher temperature phase transitions the images could be made considerably stronger in the case of the higher temperature satellites and these were therefore preferred. The highest temperature at which a stranded image could be obtained was about 100 K. By this temperature the intensity was diminishing rapidly with further increase in temperature. Neither the strand dimensions nor the fringe spacing changed with temperature in the range 30–100 K.

The second important point is that the images were found to be time dependent with different rates of evolution above and below the lower temperature phase transition. On cooling below 40 K the images were observed to be in a state of constant movement with individual strands lighting up, branching, or vanishing in fractions of a second ("twinkling"). Special techniques were developed to record the development of the images with time so that up to six exposures could be obtained on one piece of film with a time lapse of down to approximately one second between exposures. A very complicated picture emerges. Although the spacing of the strands appears to be much smaller in micrographs without the fringe patterns than in the regions of Fig. 1 where the fringes are visible, the time lapse pictures correct this impression. In the "strand" micrographs it is evidently the boundaries between certain of the strands which are revealed while the "fringe" micrographs reveal detail within the strands themselves. Adjacent strands interact so that at any one time the fringes may be approximately in phase over many strands for a distance of 100 nm or more. However, in a later micrograph each fringe in a patch of smooth fringes is broken up into many steps as the phase jumps

from one strand to another. The spacing between these phase jumps is about 20 nm, a distance comparable with the finest strand spacings. It seems that the relative movement of the fringes in different strands is related to the twinkling effect observed in strand images. Similar changes were also observed at temperatures above the lower phase transition but these were on a longer time scale, with several seconds between jumps. The trains of fringes in the strands are at least 2000 nm long so that the typical strand dimensions are 20×2000 nm.

In fact, a wide variety of contrast effects has been observed in SDF images, strand and fringe images representing the two extreme cases. Another feature of these images is that although bend contours, imaged in matrix reflections, were smooth, the SDF contours were irregular with discontinuous boundaries. The broken nature of the satellite contours indicates that the Bragg condition jumps discontinuously from one strand to the next and that each strand is a coherently diffracting object. The fringe spacing in a given area increases with time but apparently does not depend significantly on the crystal orientation. Typical spacings vary from about 100 nm at onset to 500 nm after a period of one hour or more. Finer fringes can sometimes be seen. These finer fringes may either exist alone in strands with spacings down to 50 nm or else appear as fine ($\sim$10 nm) modulations of the more widely spaced fringes. The resolution limit of our SDF observations is about 5 nm and fringes down to 8 nm have been recorded. Efforts to resolve the splitting of the satellite reflections have proved fruitless on the whole. Long exposure, selected area diffraction experiments with very long camera lengths and very small angular divergence of the illumination are required. These conditions are hard to meet in the circumstances of our experiments. However, when a region of crystal with 50 nm fringes was investigated the diffraction pattern revealed doubling of the spots in the direction of $\vec{q}$ in addition to slight streaking in a direction perpendicular to $\vec{q}$. The perpendicular streaking, implying rotations of $\vec{q}$ by up to about 15° from the b^* axis, was frequently encountered. For the larger fringe spacings observed the fractional change in magnitude called for is $\Delta q/q \sim \frac{1}{100}$, while the finer fringes require larger changes $\Delta q/q \sim \frac{1}{10}$.

The jumps in contrast along the edge of a bend contour could arise for a variety of reasons, the two most likely being the existence of elastic strain fields that vary from one strand to another, or a variation of the charge-density-wave vector ($\vec{q}$) within each strand. If $\vec{q}$ does indeed differ somewhat from one strand to another then the trains of fringes within each strand are likely to be Moiré effects between two slightly different $\vec{q}$ values within the thickness of the sample. As the fringes were observed at temperatures both above and below the lower temperature phase transition they cannot be the result of interaction between the two different CDW's. Also, as the micrographs recorded above and below the lower temperature phase transition were essentially indistinguishable their explanation has to rely solely on the higher temperature CDW's. It seems reasonable to suppose that the transverse dimensions of the strands are isotropic (see Fig. 2) and as the whisker thickness in Fig. 1 is approximately 50 nm it follows that these images could result from the projection of effects from two strands. Apparently related effects are well known in the transmission electron microscopy of long-range ordered superstructures. Very widely spaced Moiré fringes have been found as a result of composition fluctuations in the Nowotny phases and nominally stoichiometric Ta_2O_5. Moiré fringes could arise from changes in either the magnitude or the direction of $\vec{q}$, and our evidence indicates that both these effects occur in $NbSe_3$.

If this interpretation is correct the relative slippage of fringes in the strands might result from the relative displacement (or sliding motion) of charge density waves in adjoining strands. If the slippage were between charge density waves in strands lying one on top of the other within the thickness of the specimen the fringe motion would be magnified by the Moiré effect. However, without a more detailed model one cannot deduce the mobility of the charge density waves themselves

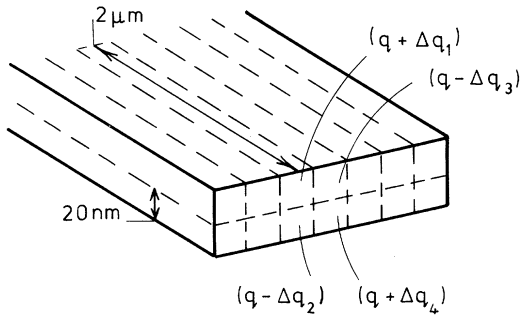

FIG. 2. Schematic diagram illustrating a model which could account for the experimental observations.

from these observations.

The model which is suggested by these observations for the higher transition temperature CDW state in $NbSe_3$ is illustrated in Fig. 2. The whisker is broken up into weakly interacting strands with typical dimensions indicated in the diagram. Each strand differs from its neighbors in having a slightly different CDW vector, with variations in the magnitude of $\vec{q}$ coupled with small changes in its direction. The waves in the strands are able to slide past each other without much resistance.

It is not clear at present why the fringes move and the strands twinkle. No electric field has been deliberately applied. However, the chief energy loss of the high-energy electron traversing the sample will be in plasmon excitation and we have in fact recorded plasmon loss spectra from some of these samples as they were cooled in the electron microscope. These high-energy collective excitations are presumably all that is required to unpin the charge density waves. Subsequent drift could then occur under the influence of charging fields which are always present in TEM, chiefly as a result of secondary electron emission from the irradiated regions of the specimen. Alternatively, a thermal gradient in the sample might be responsible.

An interesting point arises in connection with the paper by Lee and Rice on the unpinning of CDW's. They draw a distinction between weak and strong pinning and conclude that charged impurities would give rise to a strong pinning effect. The strands observed in this work contain approximately 4×10^7 atoms so that, for an impurity concentration of one in 10^4, there would be approximately 4000 impurities per strand. This number points to a weak pinning mechanism so that either the concentration of charged impurities is very low, which seems unlikely, or else the values they assumed for the coherence lengths were too small. In order to explain the movement of strongly pinned CDW's under the influence of small electric fields Lee and Rice[6] proposed a dislocation model by analogy with the need for crystal dislocations to explain the mechanical weakness of metals against plastic deformation. We do indeed observe dislocations in the fringe patterns reported here but they remain static while the fringes in individual strands slide through them. This point is illustrated schematically in Fig. 3.

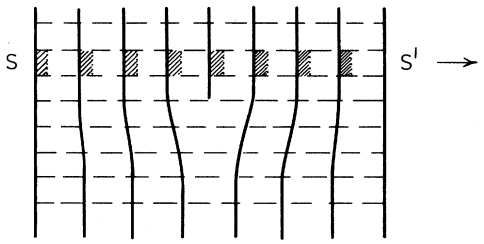

FIG. 3. Schematic diagram illustrating the sliding of fringes past a static fringe dislocation. Solid lines indicate the crests of the waves; broken lines indicate the strands. The dotted portion of strand SS' indicates the position of the crests in this strand at a later time and the shading represents the areas swept by the crests.

We have benefited from several stimulating conversations with Dr. Eades, Dr. Gill, Dr. Gyorffy, and Dr. Wilson which we gratefully acknowledge. This work was supported in part by a grant from the Science Research Council.

[1]J. A. Wilson, Phys. Rev. B 19, 6456 (1979).
[2]N. P. Ong and P. Monceau, Phys. Rev. B 16, 3443 (1977).
[3]J. C. Gill, J. Phys. F 10, L81 (1980).
[4]J. L. Hodeau, M. Marezio, C. Roucau, R. Ayroles, A. Meerschaut, J. Rouxel, and P. Monceau, J. Phys. C 11, 4117 (1978).
[5]R. M. Fleming, D. C. Moncton, and D. B. McWhan, Phys. Rev. B 18, 5560 (1978).
[6]P. A. Lee and T. M. Rice, Phys. Rev. B 19, 3970 (1979).

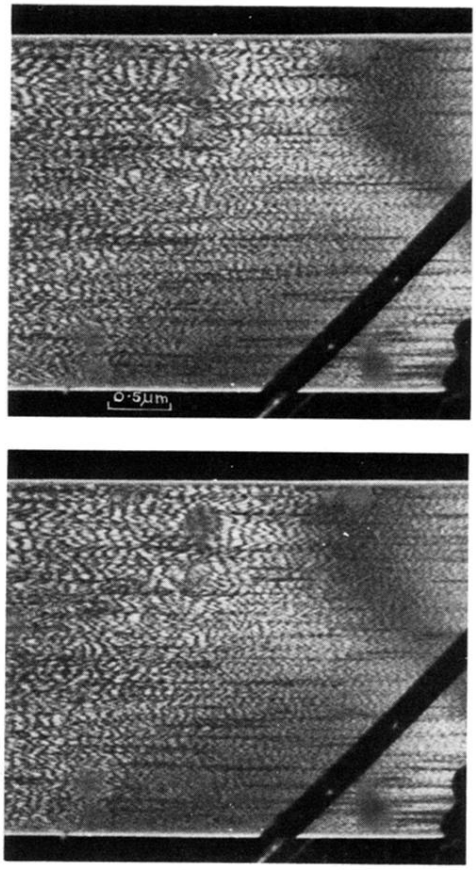

FIG. 1. Images revealing strands parallel to the whisker axis (right-hand sides of the micrographs) and trains of fringes within the strands (left-hand sides). The micrographs were two-second exposures taken with a time interval of approximately one minute. The dark band is the shadow of another whisker.